Coulomb Blockade in a Two-Dimensional Conductive Polymer Monolayer

M. Akai-Kasaya,[1,*] Y. Okuaki,[1] S. Nagano,[2] T. Mitani,[3] and Y. Kuwahara[1]
[1]*Precision Science and Technology, Graduate School of Engineering, Osaka University, 2-1 Yamadaoka, Suita, Osaka 565-0871, Japan*
[2]*Nagoya University Venture Business Laboratory, Graduate School of Engineering, Nagoya University, Furo-cho, Chikusa-ku, Nagoya 464-8601, Japan*
[3]*Japan Advanced Institute of Sciene and Technology, 1-1 Asahidai, Nomi, Ishikawa 923-1292, Japan*
(Received 20 May 2015; published 4 November 2015)

Electronic transport was investigated in poly(3-hexylthiophene-2,5-diyl) monolayers. At low temperatures, nonlinear behavior was observed in the current-voltage characteristics, and a nonzero threshold voltage appeared that increased with decreasing temperature. The current-voltage characteristics could be best fitted using a power law. These results suggest that the nonlinear conductivity can be explained using a Coulomb blockade (CB) mechanism. A model is proposed in which an isotropic extended charge state exists, as predicted by quantum calculations, and percolative charge transport occurs within an array of small conductive islands. Using quantitatively evaluated capacitance values for the islands, this model was found to be capable of explaining the observed experimental data. It is, therefore, suggested that percolative charge transport based on the CB effect is a significant factor giving rise to nonlinear conductivity in organic materials.

DOI: 10.1103/PhysRevLett.115.196801 PACS numbers: 73.23.Hk, 73.61.Ph, 74.20.Pq

The interface between an organic semiconductor and a dielectric layer plays a critical role in carrier transport in organic field-effect transistors (OFETs), because the intrinsic transport characteristics are governed by only a few molecular layers at the interface. Good organic conductors often have a low-dimensional configuration, e.g., quasi-one-dimensional (1D) structures or two-dimensional (2D) layers. Nevertheless, a large number of fundamental questions remain to be answered regarding the charge-transport mechanism, particularly in low-dimensional structures.

One such question concerns the nonlinear behavior that is often observed in the current-voltage (I-V) characteristics of organic conductors. Even for materials that exhibit good linear I-V characteristics near room temperature (RT), nonlinearity can occur as the temperature is reduced, reflecting a decrease in conductivity. This effect has been interpreted using a variety of mechanisms—such as charge hopping, trapping, tunneling, and emission—either within the organic material or at the interfaces. Explanations have been proposed involving classical physical models previously developed for inorganic materials; what these explanations have in common is that the expression for the current contains an exponential term involving the electric field (E) and the temperature (T). However, the observed nonlinearity cannot be fully explained using these conventional models or combinations of them.

Recently, it has been reported that the I-V characteristics obey a power-law relationship in low-dimensional organic materials such as polymer nanofibers [1], nanotubes [2], and polymer films [3,4], as is the case for carbon nanotubes and inorganic quantum wires. The observed power-law relationship for polymer materials has been put forward as evidence for tunneling into a 1D Luttinger liquid because of the quasi-1D structure of these materials [2,3]; however, power-law behavior was also observed for a three-dimensional (3D) polymer film [4]. The origin of such power-law behavior in organic materials is still under debate [5].

On the other hand, in inorganic granular materials, the power-law dependence of the I-V characteristics has commonly been attributed to dissipative tunneling processes, such as that associated with a Coulomb blockade (CB) [6–8]. The CB effect has been confirmed during charge transport through a single molecule spanning adjacent electrodes [9,10], although it has rarely been suggested as the origin of nonlinear conduction in larger condensed organic conductor systems [4,11,12]. CB transport occurs in systems consisting of an array of small conductive islands connected by narrow junctions, provided the tunneling resistance between neighboring sites is significantly larger than the quantum resistance ($\gg h/e^2$), the capacitance associated with each island is sufficiently small, and the energy corresponding to an additional electron charge at each site is large compared to k_BT. Here, h is Planck's constant, e is the charge of an electron, and k_B is Boltzmann's constant. Since the nature of the individual sites (i.e., whether they are metallic, superconducting, or semiconducting) is irrelevant [13], there is no reason why the CB effect should not emerge in organic materials that consist of small conducting segments.

In the present Letter, an investigation into charge transport is carried out through a 2D conjugated polymer

monolayer. The nonlinear current observed at low temperatures is found to be consistent with charge transport associated with the CB effect in an array of small conducting islands (CB array). The extended charge carrier state in a π-stacked polymer is calculated, and a structural model is proposed for a 2D CB array in a conjugated polymer monolayer. Estimates of the capacitance and CB parameters using this model suggest the validity of percolative charge transport based on the CB effect.

The organic conductor used in the present study was highly ordered poly(3-hexylthiophene-2,5-diyl) (P3HT), which is one of the most common organic polymers used in OFETs. The regioregularity-induced lamellar P3HT chains have a strong tendency to stack together ($\pi - \pi*$ stacking) and eventually form a 2D sheet. A liquid-crystal hybridized Langmuir Blodget method [14] was used to prepare an ideally spread monolayer consisting of uniaxially aligned P3HT lamellae on a water surface, and the layer was then transferred to a solid substrate.

The monolayer appeared homogeneous and isotropic in atomic-force microscopy images, although structural anisotropy was clearly identified by polarized absorption spectroscopy, grazing-incidence x-ray diffraction [14], and electron spin resonance [15]. To carry out electrical measurements, we used metal electrodes embedded in a SiO_2 layer grown on a Si substrate and with a thickness of 100–300 nm, as shown in Fig. 1(a). In order to minimize distortion of the molecular film, the electrode surface was planarized by mechanical polishing [16] until the height difference between it and the SiO_2 was less than 3 nm. The P3HT monolayer was transferred onto the substrate with the electrodes, with the molecular lamellae aligned along the channel direction. In this study, more than 50 samples were investigated, with channel length (L) and width (W) varying in the range 100–600 nm and 250–2000 nm, respectively. Measurements were carried out using a variable temperature probe (TPP-4, Lakeshore Co., Ltd.) and a semiconductor characterization system (Keithley 4200) in a vacuum of about 1×10^{-5} Pa under dark conditions. The samples were found to behave as bottom-contact FET devices, and exhibited good p-channel characteristics with a charge mobility of

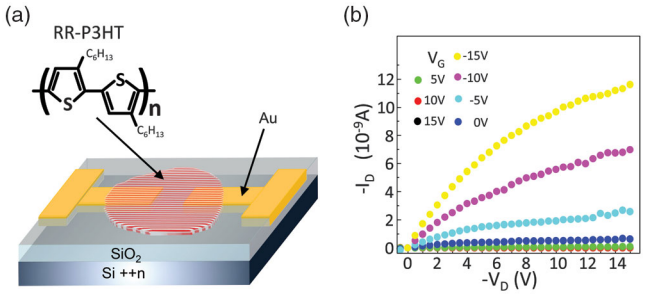

FIG. 1 (color). (a) Schematic view of planar gold electrodes covered by a P3HT monolayer. (b) Typical field-effect transistor (FET) characteristics of the P3HT monolayer, for a sample with $L = 200$ nm and $W = 500$ nm.

0.001–0.1 $cm^2/V\,s$. Typical FET characteristics are shown in Fig. 1(b). The temperature dependence of the contact resistance was investigated for a device with multiple channels with different lengths. Although the contact resistance at room temperature was high, and comparable to the resistance of the P3HT monolayer, the ratio of the contact resistance to the total resistance decreased dramatically with decreasing temperature because of the large increase in film resistivity. At lower temperatures, where the CB effect apparently emerges, the charge-transport properties are dominated by the P3HT monolayer, with a negligible contribution from the contacts. Detailed experimental conditions are described in the Supplemental Material [17].

The current flowing through the P3HT monolayer between two electrodes was basically measured without deliberately applying any gate bias voltage (V_G) at temperatures from RT to 4.2 K. Figure 2(a) shows the I-V characteristics. It can be seen that the current decreases rapidly with temperature. The lower pane in Fig. 2(a) shows the I-V curves for temperatures of 150 K and lower on an expanded current scale. Clear nonlinear characteristics can be observed, and a different threshold voltage (V_T), below which no current flows, exists at each temperature. The ability to detect a current at low temperatures is due to the use of a P3HT monolayer and a short channel length. This was not possible for either a P3HT monolayer with a channel length of several microns or more, or a thicker spin-coated P3HT film with a channel length of less than one micron [17].

All of the I-V curves in the lower pane of Fig. 2(a) have the same shape, but they shift to higher voltage as the temperature decreases. Figure 2(b) shows the I-V characteristics below 150 K plotted on a double logarithmic scale, where the curves are made to coincide by subtracting the V_T values. It can be seen that at higher voltages, the data can be well fitted using a straight line, indicating a power-law relationship given by

$$I = \alpha(V - V_T)^{\xi} \tag{1}$$

with coefficients α and ξ. V_T decreases with increasing temperature as shown in the inset in Fig. 2(b), and the relationship is expressed by

$$V_T(T) = V_T(0) \times (1 - \beta T), \tag{2}$$

where $V_T(0)$ is the threshold voltage at 0 K and β is a coefficient. Equations (1) and (2) describe percolative charge transport in a 2D CB array, as predicted by Middleton and Wingreen [25]. The solid lines in the lower panel in Fig. 2(a) are fits using Eq. (1) with α and ξ values of 2×10^{-16} and 3.9, respectively. There is seen to be good agreement between the experimental data and the fitted curves. No better fit could be obtained using any other nonlinear charge-transport model [17].

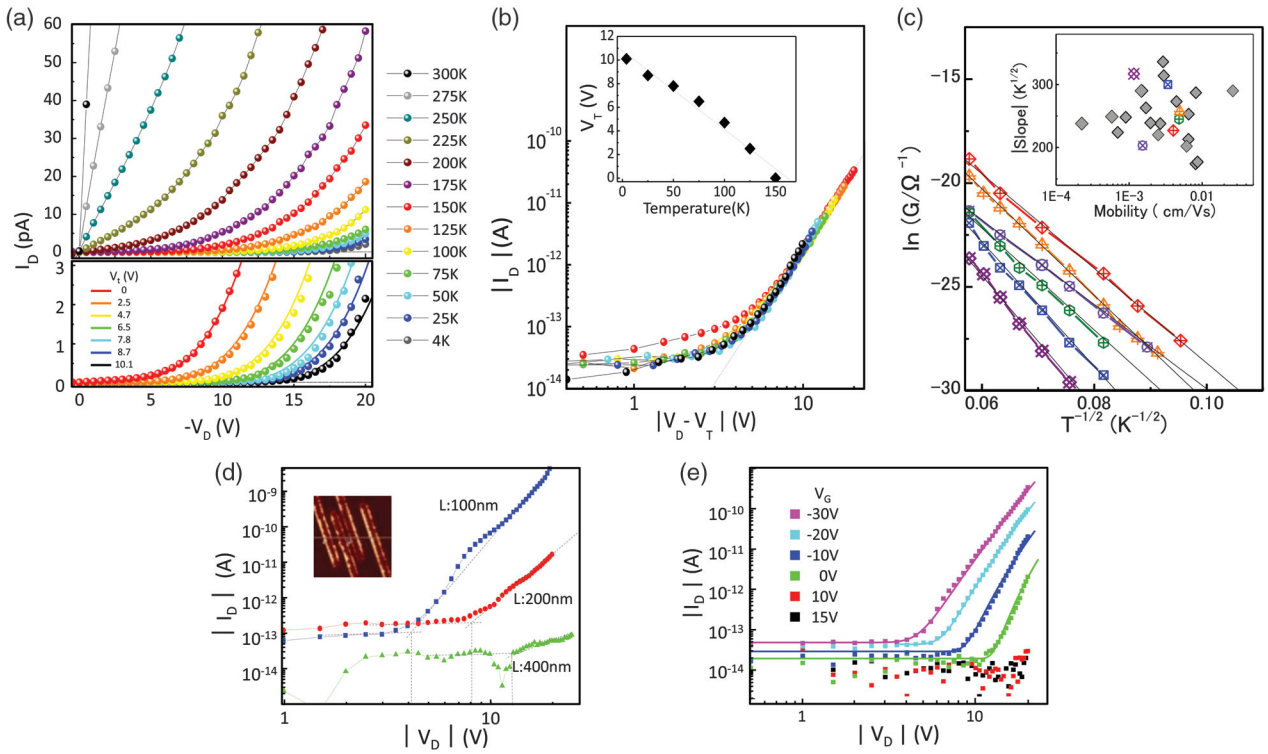

FIG. 2 (color). (a) Typical I-V characteristics from RT to 4.2 K, for a sample with $L = 500$ nm and $W = 2000$ nm. The lower chart shows data obtained below 150 K. The colored solid lines are fits using Eq. (1). (b) Low-temperature I-V curves shown on a log-log scale. The slope of the dotted line yields an exponent ξ of 3.9. The subtracted V_T values are shown in the inset. (c) $\ln(G)$ at zero bias voltage against $T^{-1/2}$ for six typical samples. The inset shows the dependence of the slope of the $\ln(G) - T^{-1/2}$ curve on the mobility at RT for 25 samples. (d) I-V curves obtained at 4.2 K for a sample with multiple channel lengths with $W = 2000$ nm. (e) I-V curves obtained at 4.2 K for sample with $L = 200$ nm and $W = 500$ nm, and different V_G values.

In the present study, three parameters are used to evaluate charge transport in a 2D CB array: $V_T(0)$, ξ, and the critical temperature ($T*$) for the blockade effect. Individual conductive islands are considered to have a self-capacitance C_0 and to be coupled together by a capacitance C_i. For thermal energy well below the charging energy, i.e., $k_BT \ll e^2/2C$, charge transfer is blocked until the potential difference between the islands is lower than the local tunneling threshold voltage. The observed V_T for such an array is the sum of that for each island that lies along the transport path. The extrapolated value of V_T at 0 K is $V_T(0)$; it provides information about the energy of the system, although it is sensitive to the array size. Furthermore, when charge carriers acquire sufficient thermal energy to overcome the local threshold, i.e., when the temperature is $T*$, V_T vanishes and a finite conductance (G) appears at zero bias voltage. Charge transport in the CB array is basically percolative. Since the number of available transport paths increases with voltage under low-power conditions, the exponent ξ depends on the dimensionality and configuration of the array [25,26]. For the approximately 30 samples in the present study, with different L and W values, $V_T(0)$ was in the range 3–12 V, $T*$ in the range 110–160 K, and ξ in the range 3.3–3.9.

The higher-temperature I-V curves, obtained from RT to $T*$, exhibit a finite $G_{V=0}$. Figure 2(c) shows $G_{V=0}$ plotted on a logarithmic scale against $T^{-1/2}$. It is noteworthy that the data closely resemble that reported for a monodisperse inorganic quantum dot (QD) array [8]. The observed linear relationship can be ascribed to an Efros-Shklovskii variable-range hopping transport mechanism [27], which takes into account Coulomb interactions. The inset in Fig. 2(c) shows the slope of the $\ln(G)$-$T^{-1/2}$ curves plotted against mobility at RT. For the inorganic QD array, the slope of $\ln(G)$-$T^{-1/2}$ was found to depend on the array dimensionality. However, for the P3HT monolayers in the present study, no clear dependence on mobility or any other parameter was found [17]. The difference between the curves in Fig. 2(c) is considered to be due to variations in the quality of the molecular film from sample to sample.

Figure 2(d) shows I-V curves obtained at 4.2 K for a device with multiple channel lengths. It is clear that V_T linearly increases as the channel length L increases. This is reasonable because V_T is the sum of the local threshold voltages along the current path, and is, thus, proportional to the channel length L. From the shape of the curves in Fig. 2(d), it is also clear that ξ (i.e., the incline of current increase) decreases as L increases. This is consistent with

the results of a recent theoretical study, in which ξ was found to depend on the aspect ratio of a 2D CB lattice [26].

Figure 2(e) shows typical I-V curves obtained at 4.2 K for different values of V_G. The V_T value is seen to decrease as V_G becomes more negative. This is reasonable because the charge carriers in P3HT are holes. A negative V_G will reduce the island potential, and, thus, the charge injection threshold will decrease. The opposite effect may occur for inorganic QDs. For QDs with a large C_0, a negative V_G is expected to increase the amount of positive charge accumulated in each island, thus blocking further hole injection. However, in organic systems with a small C_0, little charge accumulation is expected, so most islands will still be electrically neutral. Thus, a negative V_G enhances hole injection into p-type organic semiconductor QDs similar to the case for conventional field-effect charge accumulation.

The experimental results are basically consistent with percolative charge transport in a CB array. The question then arises as to the fundamental nature of the conductive islands in the P3HT monolayer. We have previously reported that P3HT monolayers with an anisotropic structure exhibited isotropic conductivity [28]. In fact, even during the low-temperature measurements performed in the present study, no anisotropic behavior was observed. To account for this, we previously proposed the concept of a random distribution of defects, as shown in Fig. 3(a). The semicrystalline structure of polymers generally comprises highly ordered domains (crystallites) and amorphous regions. The P3HT monolayer is considered to have a larger fraction of in-plane-oriented domains than that of conventional spin-coated films due to the two-dimensional confinement. Our structural model is simplified, in that it consists of a regularly stacked polymer backbone together with fatal defects in the highly ordered domains. These defects correspond to breaks in the π conjugation, i.e., the ends of polymer chains, in addition to points where tilting and bending of the molecular plane occur. Based on a relative neighborhood graph method [29], small segments with continuous π stacking were found to be bounded by these defects. Polaronic charge carriers may be energetically stable in segments that are sufficiently large, such as the colored segments in Fig. 3(a). It was concluded that 2D charge hopping is the origin of the isotropic charge transport in P3HT monolayers. However, the spatial extent of the polaronic states in the segments was still uncertain.

The electronic states were next calculated for a single positively charged π stacked polythiophene sheet cluster. The calculations were based on DFT and were carried out using the DMol3 program [20] with a 6–31 + $G**$ basis set [30]. Figure 3(b) shows the upper unoccupied orbital in a singly occupied molecular orbital. The degeneracy of the half-filled highest-occupied molecular orbital was removed, and a split occurred between the upper unoccupied and lower occupied levels. The upper unoccupied orbital corresponds to the charge state of holes in a square sheet of

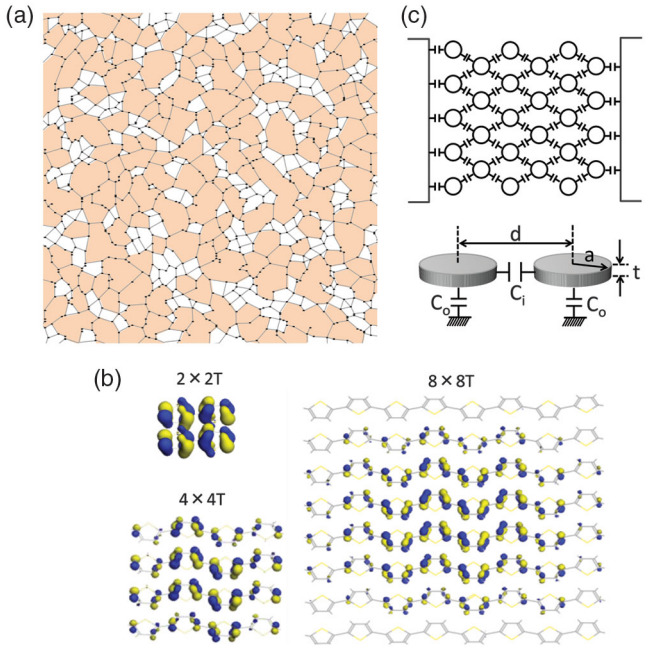

FIG. 3 (color). (a) Random defect distribution in 100×100 nm^2 area of a 2D P3HT monolayer. The defects were connected using the relative neighborhood graph method; only regions wider than a circle with a diameter of 5 nm are colored. (b) Density-functional theory (DFT) calculation results for singly occupied molecular orbitals, i.e., hole states, in $n \times nT$ sheet clusters, where n n-thiophene oligomers are stacked with a π-π distance of 0.37 nm. (c) 2D CB array model consisting of conductive disk-shaped islands. Details concerning the defect distribution simulation and DFT calculation results are provided in the Supplemental Material [17].

P3HT. It can be seen that for an $8 \times 8T$ cluster, the hole states are concentrated in a circular region near the center, whereas they extend throughout smaller clusters. The edge of the sheet cluster can be considered to be a structural defect. It was found that when a structural defect was intentionally introduced into the $8 \times 8T$ cluster, the hole states assumed an elliptical shape to avoid the defect [17]. These results indicate that the hole states in a π-stacked polythiophene sheet can extend isotropically, regardless of the polymer direction.

These results support the 2D charge-hopping model in an array of small segments with continuous π stacking in a P3HT monolayer. This array could be regarded as the equivalent of a CB array, which consists of conductive islands and charge tunneling barriers, as shown in Fig. 3(c). In this study, the CB parameters $V_T(0)$ and $T*$ were estimated for a P3HT monolayer assuming an array of conductive disks with a radius a, a thickness t, and a spacing d, as shown in Fig. 3(c). Details are provided in the Supplemental Material [17]. For an array of N^2 disks with a, t, and d values of 1.5, 0.01, and 6 nm, respectively, the elemental threshold voltage $[V_T(0)/N]$ is estimated to be 0.059 63 eV. For the case of electrodes with a separation of 100 nm, $N = 19$, and the measured $V_T(0)$ is then expected to be about 1.13 V. At the

critical temperature, the simple relation $k_B T* = eV_T(0)/N$ holds. However, at a finite temperature, the charges must have a Fermi-Dirac energy distribution. Such thermal energy considerations have been discussed in relation to percolative transport by Elteto *et al.* for a 2D triangular array [31]. Based on their approximation and the energy distribution, $T*$ was estimated to be about 111 K.

In the present study, the measured $V_T(0)$ and $T*$ values for samples with a channel length of 100 nm were 2.8–4.8 V and 110–160 K, respectively. The estimated values using the simple model described above are in reasonably good agreement with the experimentally measured values, although the calculated $V_T(0)$ was smaller than the experimental values. This supports the idea that CB-type charge transport can occur in P3HT monolayers. The model used in the present study was simplistic, and did not take into account factors such as the structural deformation energy or chemical redox effects in organic materials, which are also likely to block incoming charges. Also, the existence of the underlying dielectric layer might affect the intrinsic capacitance of each island. It should also be noted that these additional mechanisms would be expected to change the critical energy for charge blocking, and could, therefore, potentially be taken into account by changing the capacitance values in the CB array model.

The importance of the present results is that percolative charge transport may well explain experimentally observed charge transport in low-dimensional organic materials. The significance of the blockade effect, i.e., the difficulty of charge injection from one conducting segment into another, should also be stressed, since this has not hitherto been taken into account when considering the charge-transport mechanism in organic materials. Conductive segments in poorly conductive organic materials are expected to have a smaller electrical capacity, leading to a higher $T*$ for the blockade effect. The presence of structural disorder in organic materials will obscure the emergence of a distinguishable conduction threshold; ironically, though, such disorder is a requirement for percolative transport. By considering both the charge-blockade effect and the influence of structural disorder, it is hoped that a clear understanding of charge transport in organic materials can be achieved.

This work is supported by a Grant-in-Aid for Scientific Research (S) (No. 24221009) and Grant-in-Aid for Scientific Research on Innovative Areas "Molecular Architectonics: Orchestration of Single Molecules for Novel Functions" from the Ministry of Education, Culture, Sports, Science and Technology, Japan.

*kasaya@prec.eng.osaka-u.ac.jp

[1] A. N. Aleshin, H. J. Lee, Y. W. Park, and K. Akagi, One-Dimensional Transport in Polymer Nanofibers, Phys. Rev. Lett. **93**, 196601 (2004).

[2] A. Rahman and M. K Sanyal, Bias dependent crossover from variable range hopping to power law characteristics in the resistivity of polymer nanowires, J. Phys. Condens. Matter **22**, 175301 (2010).

[3] J. D. Yuen, R. Menon, N. E. Coates, E. B. Namdas, S. Cho, S. T. Hannahs, D. Moses, and A. J. Heeger, Nonlinear transport in semiconducting polymers at high carrier densities, Nat. Mater. **8**, 572 (2009).

[4] A. J. Kronemeijer, E. H. Huisman, I. Katsouras, P. A. van Hal, T. C. T. Geuns, P. W. M. Blom, S. J. van der Molen, and D. M. de Leeuw, Universal Scaling in Highly Doped Conducting Polymer Films, Phys. Rev. Lett. **105**, 156604 (2010).

[5] A. S. Rodin and M. M. Fogler, Apparent Power-Law Behavior of Conductance in Disordered Quasi-One-Dimensional Systems, Phys. Rev. Lett. **105**, 106801 (2010).

[6] R. Parthasarathy, X.-M. Lin, and H. M. Jaeger, Electronic Transport in Metal Nanocrystal Arrays: The Effect of Structural Disorder on Scaling Behavior, Phys. Rev. Lett. **87**, 186807 (2001).

[7] H. Fan, K. Yang, D. M. Boye, T. Sigmon, K. J. Malloy, H. Xu, G. P. López, and C. J. Brinker, Self-assembly of ordered, robust, three-dimensional gold nanocrystal/silica arrays, Science **304**, 567 (2004).

[8] K. Xu, L. Qin, and J. R. Heath, The crossover from two dimensions to one dimension in granular electronic materials, Nat. Nanotechnol. **4**, 368 (2009).

[9] S. Kubatkin, A. Danilov, M. Hjort, J. Cornil, J.-L. Brédas, N. Stuhr-Hansen, P. Hedegård, and T. Bjørnholm, Single-electron transistor of a single organic molecule with access to several redox states, Nature (London) **425**, 698 (2003).

[10] J. Park, A. N. Pasupathy, J. I. Goldsmith, C. Chang, Y. Yaish, J. R. Petta, M. Rinkoski, J. P. Sethna, H. D. Abruña, P. L. McEuen, and D. C. Ralph, Coulomb blockade and the Kondo effect in single-atom transistors, Nature (London) **417**, 722 (2002).

[11] A. N. Aleshin, H. J. Lee, S. H. Jhang, H. S. Kim, K. Akagi, and Y. W. Park, Coulomb-blockade transport in quasi-one-dimensional polymer nanofibers, Phys. Rev. B **72**, 153202 (2005).

[12] Y. Hirano,Y. Segawa, T. Kawai, and T. Matsumoto, Stochastic resonance in a molecular redox circuit, J. Phys. Chem. C **117**, 140 (2013).

[13] *Single Charge Tunneling: Coulomb Blockade Phenomena in Nanostructures*, edited by H. Grabert and M. H. Devoret, NATO ASI Series Vol. 294 (Plenum, New York, 1992), p. 139.

[14] S. Nagano, S. Kodama, and T. Seki, Ideal spread monolayer and multilayer formation of fully hydrophobic polythiophenes via liquid crystal hybridization on water, Langmuir **24**, 10498 (2008).

[15] S. Watanabe, H. Tanaka, S. Kuroda, A. Toda, S. Nagano, T. Seki, A. Kimoto, and J. Abe, Electron spin resonance observation of field-induced charge carriers in ultrathin-film transistors of regioregular poly(3-hexylthiophene) with controlled in-plane chain orientation, Appl. Phys. Lett. **96**, 173302 (2010).

[16] Y. Higuchi, N. Ohgami, M. Akai-Kasaya, A. Saito, M. Aono, and Y. Kuwahara, Application of simple mechanical polishing to fabrication of nanogap flat electrodes, Jpn. J. Appl. Phys. **45**, L145 (2006).

[17] See Supplemental Material at http://link.aps.org/supplemental/10.1103/PhysRevLett.115.196801 for details about sample preparation, calculation and measurement results are described, which includes Refs. [18–24].
[18] J. H. Wei, Y. L. Gao, and X. R. Wang, Inverse square-root field dependence of conductivity in organic field-effect transistors, Appl. Phys. Lett. **94**, 073301 (2009).
[19] T. Izumi, S. Kobashi, K. Takimiya, Y. Aso, and T. Otsubo, Synthesis and spectroscopic properties of a series of β-blocked long oligothiophenes up to the 96-mer: Revaluation of effective conjugation length, J. Am. Chem. Soc. **125**, 5286 (2003).
[20] B. Delley, An all-electron numerical method for solving the local density functional for polyatomic molecules, J. Chem. Phys. **92**, 508 (1990); B. Delley, From molecules to solids with the $DMol^3$ approach, J. Chem. Phys. **113**, 7756 (2000).
[21] J. P. Perdew, K. Burke, and M. Ernzehof, Generalized Gradient Approximation Made Simple, Phys. Rev. Lett. **77**, 3865 (1996); J. P. Perdew and Y. Wang, Accurate and simple analytic representation of the electron-gas correlation energy, Phys. Rev. B **45**, 13244 (1992).
[22] *Handbook of Conductive Polymers*, 2nd ed., edited by T. A. Skotheim, R. L. Elsenbaumer, and H. J. R. Reynolds (Marcel Dekker, Inc., New York, 1998).
[23] NIMS PolyInfo, http://polymer.nims.go.jp/.
[24] R. Parthasarathy, X.-M. Lin, K. Elteto, T. F. Rosenbaum, and H. M. Jaeger, Percolating through Networks of Random Thresholds: FiniteTemperature Electron Tunneling in Metal Nanocrystal Arrays, Phys. Rev. Lett. **92**, 076801 (2004).
[25] A. A. Middleton and N. S. Wingreen, Collective Transport in Arrays of Small Metallic Dots, Phys. Rev. Lett. **71**, 3198 (1993).
[26] T. Narumi, M. Suzuki, Y. Hidaka, and S. Kai, Size dependence of current-voltage properties in coulomb blockade networks, J. Phys. Soc. Jpn. **80**, 114704 (2011).
[27] A. L. Efros and B. I. Shklovskii, Coulomb gap and low temperature conductivity of disordered systems, J. Phys. C **8**, L49 (1975).
[28] M. Akai-Kasaya, Y. Okuaki, S. Nagano, A. Saito, M. Aono, and Y. Kuwahara, Isotropic charge transport in highly ordered regioregular poly(3-hexylthiophene) monolayer, J. Phys. D **46**, 425303 (2013).
[29] G. T. Toussaint, The relative neighbourhood graph of a finite planer set, Pattern Recognition **12**, 261 (1980).
[30] D. M. Whitfield, D. Lamba, T.-H. Tang, and I. G. Csizmadia, Binding properties of carbohydrate sulfamates based on ab initio 6–31 + G^{**} calculations on *N*-methyl and *N*-ethyl sulfamate anions, Carbohydr. Res. **286**, 17 (1996).
[31] K. Elteto, E. G. Antonyan, T. T. Nguyen, and H. M. Jaeger, Model for the onset of transport in systems with distributed thresholds for conduction, Phys. Rev. B **71**, 064206 (2005).